Journal of Orthopaedic Translation 30 (2021) 70–81

Contents lists available at ScienceDirect

Journal of Orthopaedic Translation

journal homepage: www.journals.elsevier.com/journal-of-orthopaedic-translation

Original article

The effect of traumatic brain injury on bone healing from a novel exosome centered perspective in a mice model

Chengyuan Yang [a,1], Cheng Gao [b,1], Naicheng Liu [a,1], Yitong Zhu [d], Xu Zhu [a], Xinlin Su [a], Qin Zhang [a], Yanglin Wu [a], Chenhui Zhang [a], Ang Liu [a], Weifeng Lin [c], Luyang Tao [b,**], Huilin Yang [a,***], Jun Lin [a,*]

[a] Department of Orthopaedic Surgery, The First Affiliated Hospital of Soochow University, Suzhou, China
[b] Department of Forensic Medicine, Soochow University, Suzhou, China
[c] Department of Materials and Interfaces, Weizmann Institute of Science, Rehovot, 76100, Israel
[d] Suzhou Key Laboratory for Medical Biotechnology, Suzhou Vocational Health College, Suzhou, China

ARTICLE INFO

Keywords:
Traumatic brain injury
Bone healing
Exosomes
Liposomes
Osteoblasts
miRNAs

ABSTRACT

Background: In patients with traumatic brain injury (TBI) combined with long bone fracture, the fracture healing is always faster than that of patients with single fracture, which is characterized by more callus growth at the fracture site and even ectopic ossification. Exosomes are nanoscale membrane vesicles secreted by cells, which contain cell-specific proteins, miRNAs, and mRNAs.

Methods: In this study, we used exosomes as the entry point to explore the mechanism of brain trauma promoting fracture healing. We established a model of tibia fracture with TBI in mice to observe the callus growth and expression of osteogenic factors at the fracture site. Blood samples of model mice were further collected, exosomes in plasma were extracted by ultra-centrifugation method, and then identified and acted on osteoblasts cultured in vitro. The effects of exosomes on osteoblast differentiation at the cell, protein and gene levels were investigated by Western Blot and q-PCR, respectively. Furthermore, miRNA sequencing of exosomes was performed to identify a pattern of miRNAs that were present at increased or decreased levels.

Results: The results suggested that plasma exosomes after TBI had the ability to promote the proliferation and differentiation of osteoblasts, which might be due to the increased expression of osteoblast-related miRNA in exosomes. They were transmitted to the osteoblasts at the fracture site, so as to achieve the role of promoting osteogenic differentiation.

Conclusion: The TBI-derived exosomes may have potential applications for promoting fracture healing in future.

The Translational Potential of this Article: Plasma exosomes early after TBI have the ability to promote osteoblast proliferation and differentiation. The mechanism may be achieved by miRNA in exosomes. Plasma exosomes may be used as breakthrough clinical treatment for delayed or non-union fractures.

1. Introduction

Traumatic brain injury (TBI) with limb fractures usually occurs in high-energy injuries, such as traffic accident injuries. In the 1960s, Gilbson reported a large amount of callus formation at the fractured end of TBI patients with fractures. Clinicians have also observed that TBI can accelerate the growth of callus and increase the amount of callus, thereby accelerating fracture healing. But its exact mechanism of action has not been fully elucidated [1]. It is believed that the influence of TBI on fracture healing is jointly regulated by the internal environment of the

* Corresponding author. Department of Orthopaedic Surgery, The First Affiliated Hospital of Soochow University, 899 Pinghai Road, Suzhou, Jiangsu, 215006, China.
** Corresponding author. Department of Forensic Medicine, Medical School of Soochow University, 178 East Ganjiang Road, Suzhou, 215213, China.
*** Corresponding author. Department of Orthopaedic Surgery, The First Affiliated Hospital of Soochow University, 899 Pinghai Road, Suzhou, Jiangsu 215006, China.
E-mail addresses: taoluyang@suda.edu.cn (L. Tao), suzhouspine@163.com (H. Yang), linjun@suda.edu.cn (J. Lin).
[1] These authors contributed equally to this work and should be considered co-first authors

https://doi.org/10.1016/j.jot.2021.09.003
Received 7 April 2021; Received in revised form 12 September 2021; Accepted 13 September 2021

body and the local microenvironment of the fracture. Humoral factors play an important role in the promotion of fracture healing by TBI [2]. Brain trauma leads to the destruction of the blood–brain barrier, and brain tissue releases a series of cytokines, including bone morphogenetic protein (BMP) [3], basic fibroblast growth factor (bFGF) [4], vascular endothelial cell growth factor (VEGF) [5], etc., are transmitted to the fractured end through body fluids. On the one hand, they can directly enhance proliferation and differentiation of osteoblasts, matrix synthesis and calcification, and increase local blood circulation. On the other hand, they can accelerate bone healing by upregulating cytokines that regulate bone metabolism in the fracture area.

Exosomes are small membrane vesicles with a lipid bilayer membrane structure that can be secreted by most cells and are about 30–150 nm in diameter [6]. Exosomes were first discovered on sheep's reticulocytes in 1987. At that time, they were considered as excretory channels for transferrin receptors, and were subsequently found in peripheral blood, cerebrospinal fluid, urine and other body fluids. Exosomes contain cell-specific proteins, miRNA, and mRNA, which can be transmitted to other cells as signal molecules to affect their function. Exosomes from different cell sources have different functions. Osteoblasts are differentiated from bone marrow mesenchymal stem cells, and the secreted exosomes promoted the differentiation of osteoblasts by activating EIF2 signaling pathway [7]. Exosomes secreted by osteoblasts can also activate the RANKL–RANKL signaling pathway to regulate osteoclast differentiation [8]. Exosomes secreted by osteoclast precursor cells can promote osteoclast differentiation, while exosomes secreted by mature osteoclasts inhibit osteoclast differentiation [9].

Therefore, we propose a hypothesis that plasma exosomes with TBI play an important role in promoting fracture healing. To this end, we established a mouse model of tibia fracture combined with brain trauma, extracted plasma exosomes and co-cultured them with osteoblasts to explore the effect of exosomes on osteoblasts after brain trauma. We have also sequenced the miRNAs of these exosomes to further probe into their possible mechanism of action and provide new ideas and theoretical basis for clinical treatment of delayed or non-union fractures.

2. Materials and methods

2.1. Animals

8-week-old male C57BL/6J mice weighting 22–25 g were selected as subjects. All mice were fed with food and water ad libitum and raised in the specific pathogen-free (SPF) animal experiment room under conditions of controlled temperature (23 ± 1 °C) and humidity (55 ± 10%) on a 12h light/dark cycle. The official animal approval license number is SYXK(Su)2017–0043.

2.2. Induction of TBI combined with tibia fracture model and design of experiment

After 1 week of acclimatization, mice were randomly assigned to two groups (N = 16/group): (1) TF: TBI + F, traumatic brain injury combined with tibia fracture; (2) SF: Sham-TBI + F, performed relevant surgical procedures without damaging the brain parenchyma, but with tibia fracture.

The model was performed under anesthesia of 1% pentasorbital sodium (50 mg/kg, intraperitoneally) and every effort was made to minimize suffering. During revival period in full anesthesia, body temperature of mice was maintained at 37 °C with a heating pad.

TBI model: A craniotomy of approximately 3.5 mm in diameter was performed on mice on the right parietal cortex between bregma and lambda 1 mm from the midline using a portable drill. The dura mater was kept intact. A cone with a tip diameter of 3 mm and a weight of 20 g was used to strike the mouse brain at a height of 30 cm at a free-fall speed to induce injury.

Sham-TBI model: Suture the wound after a craniotomy of approximately 3.5 mm in diameter was performed on mice without damaging the brain parenchyma.

Tibia Fracture model: A longitudinal skin incision was made in the middle of the front of the left knee joint of the mouse to expose the patellar ligament, the patellar ligament was cut longitudinally, and the tibial plateau was exposed. After opening with the needle tip of the syringe, a needle with a diameter of 0.3 mm was inserted. Then expose the middle tibia and make a transverse fracture with sharp scissors. 80,000 U of penicillin was injected intraperitoneally for 3 consecutive days to prevent wound infection.

2.3. Radiologic analysis for bone union

Radiographic imaging was performed at 3 (n = 9/group) and 5 (n = 7/group) weeks after fracture. The left tibia specimens of 9 mice in each group were randomly collected 3 weeks after the operation, and the remaining 7 specimens were collected 5 weeks later. After taking X-rays of the specimens, the intramedullary nails were taken out and then scanned by Micro-CT scan (Skyscan 1176). Three-dimensional CT images were recreated by NRecon, DataViewer, CTAn, and Mimics software followed by analysis of the following parameters: bone volume (BV), total volume (TV), bone volume fraction (BV/TV) and trabecular number (Tb.N).

2.4. Histological evaluation

The tibial specimens of mice were examined by histopathology after imaging analysis at 3 weeks and 5 weeks after surgery. Specimens were soaked in 4% paraformaldehyde for 48 h, decalcified in 10% EDTA for 3 weeks, and embedded in wax blocks. The tibias were longitudinally cut into 5 mm thick slices and analyzed for histological differences using hematoxylin-eosin staining.

2.5. Immunohistochemical analysis

First, paraffin-embedded tibial slices were dewaxed in xylene, and then rehydrated in ethanol and water. After washing with PBS, the sections were blocked with 10% serum at room temperature for 20 min. Anti-RUNX2 (ab192256, abcam, USA) and Anti-Osterix (ab209484, abcam, USA) antibodies were added and incubated at 4 °C overnight. After washing with phosphate-buffered saline, the secondary antibody was incubated for 30 min at room temperature. DAB coloring solution was added dropwise in the dark for 5 min. The reaction was stopped by washing with deionized water. Afterwards, hematoxylin staining solution was added for 2 min. Observe under a microscope after being transparent and mounted.

2.6. Isolation of exosomes and identification of exosome markers

45 mice were randomly divided into 3 groups, normal group (NOR), TBI + Fracture group (TF), sham-TBI + Fracture group (SF), 15 mice in each group. On the 1st, 3rd, and 7th days after modeling, 1 ml of blood was obtained by abdominal aortic puncture and blood sampling from five mice in each group. Blood samples were added to EDTA anticoagulation tubes and centrifuged for 30min (3500g, 4 °C) to collect plasma. The ultracentrifugation method was used to separate the exosomes in the plasma. When the temperature of the centrifuge was reduced to 4 °C, the following steps were performed in sequence: (1) 10 min at 300g, take the supernatant; (2) 10 min at 2000g, take the supernatant; (3) 30 min at 10000g, take the supernatant; (4) Pass the supernatant through a 0.22 μm filter to further remove impurities; (5) 70min at 100000g, take the precipitate; (6) Resuspend the pellet in PBS and centrifuge again at 100,000g for 70min. The resulting precipitate is the exosome. After resuspending with a small amount of PBS, aliquot and store at −80 °C.

Transmission electron microscope (Tecnai G2 spirit BioTwin, FEI, USA) was used to observe the morphology of exosomes. Nanoparticle

Tracking Analysis (NTA) was used to analyse the size distribution and concentration of exosomes by ZetaView (Particle Metrix, Germany). In addition, Western Blot was used to detect the expression of exosome marker proteins TSG101 and CD9.

2.7. Cell culture

MC3T3-E1 cell line was obtained from the Cell Bank of the Chinese Academy of Sciences (Shanghai, China) and maintained in α-Modified Eagle's Medium (α-MEM, SH30265.01, Hyclone, USA) with 10% fetal bovine serum (FBS, 10099141, Gibco, USA) and 1% Penicillin-Streptomycin solution (15140–122, Gibco, USA). The MC3T3-E1 cells were cultured at 37 °C under 5% CO2, and during osteogenic induction, replace osteogenic differentiation medium (MUBMD-90021, Cyagen, USA). Cells were intervened by exosomes from different groups and divided into NOR group, TF group and SF group. Here, we introduce the control group (CTRL, without exosomes intervention) as a blank control.

2.8. Immunofluorescence

MC3T3-E1 cells were washed 3 times with PBS, fixed with 10% paraformaldehyde for 10 min, and then permeabilized with 1% TritonX-100 (Sigma–Aldrich) in PBS for 5 min. After blocking in staining blocking buffer (Beyotime) for 1 h, the cells were incubated with primary antibodies against RUNX2 (1: 500) or COL1A1 (1: 500) at 4 °C overnight. The nuclei were counterstained with 4′6-diamidino-2-phenylindole (DAPI) (Thermo Fisher Scientifc) for 5 min in the dark at room temperature. Use Olympus IX51 microscope (Olympus) to observe the image.

2.9. Western blotting of osteogenesis associated markers

Samples were sonicated and homogenized in the buffer (RIPA with protease cocktail inhibitor, phosphatase inhibitor, and phenylmethanesulfonyl fluoride), and assayed for protein levels of TSG101, CD9, COL1A1 and RUNX2. Protein concentration was determined with a BCA protein assay kit (P0012, Beyotime, China). Samples (10 μg protein each) were separated by 10% SDS-PAGE, transferred to PVDF membranes (Millipore, Billerica, USA), and incubated in blocking buffer [5% BSA in Tris-buffered saline (TBS) with 0.1% Tween 20] for 1 h. Membranes were then incubated overnight at 4 °C with rabbit anti-TSG101 (1:1000; 14497-1-AP, proteintech, USA), rabbit anti-CD9 (1:1000; ab223052, abcam, UK), rabbit anti-COL1A1 (1:1000; #84356, CST, USA), rabbit anti-RUNX2 (1:1000; #12556, CST, USA) and β-actin (1:3000; GB12001, Servicebio, China) antibody. The secondary incubation of membranes was in the goat anti-rabbit (1:3000; GB23303, Servicebio, China) for 1 h at room temperature. Densitometry was performed using the Bio-rad ChemiDoc Touch Imaging System.

2.10. Quantitative real-time PCR

PrimeScript™ RT Master Mix (TAKARA) was used to extract the total RNA (0.5 μl) of CTRL, NOR, TF and SF group samples and convert it to cDNA with a total capacity of 10 μl. Quantitative PCR was performed using the BioRad CFX96 Touch Real-Time Quantitative PCR system. The final reaction volume was 25 μl, and each sample used a 2 μl cDNA template. GAPDH acted as an internal control. The reaction was repeated 3 times, with at least 3 independent runs. Data analysis was performed using the ΔΔCt method Bio-Rad Ranking Manager 3.1. Primer sequences are shown in Table 1.

2.11. Alizarin Red Staining

After MC3T3-E1 cells undergo osteogenic differentiation, ARS staining was used to detect the mineralization of the extracellular matrix. The cells were washed with PBS and fixed in 4% paraformaldehyde for 15 min at room temperature. Then incubate the cells in 1% ARS solution (pH = 4.2, Sigma–Aldrich) for 15 min. An Olympus IX51 microscope (Olympus) was used to take images of matrix mineralization. Finally, 5% perchloric acid (200 μL/well, Sigma–Aldrich) was used to dissolve the staining of the calcified matrix, and a microplate spectrophotometer (BioTek) was used to measure the absorbance at 420 nm for quantitative analysis.

Table 1
Primer sequences used for the validation amongst upregulated genes.

Name	Direction	5'→3'
COL1A1	Forward	GCTCCTCTTAGGGGCCACT
	Reverse	ATTGGGGACCCTTAGGCCAT
RUNX2	Forward	GACTGTGGTTACCGTCATGGC
	Reverse	ACTTGGTTTTTCATAACAGCGGA
GAPDH	Forward	AATGGATTTGGACGCATTGGT
	Reverse	TTTGCACTGGTACGTGTTGAT

2.12. RNA-seq data processing

The exoRNeasy Serum/Plasma Maxi Kit (QIAGEN) was used to extract exosome miRNA from mouse plasma samples, and Qubit 3.0 was used to quantify the exosome miRNA. The library was constructed using Small RNA Sample Pre Kit. Small RNA had special structure at the 3′and 5′ends (complete phosphate group at 5′end and hydroxyl group at 3′end), with total RNA as the starting sample, reverse transcription synthesized cDNA. Subsequently, after PCR amplification, the target DNA fragments were separated by PAGE gel electrophoresis, and the cDNA library was recovered by excising the gel. After the library construction was completed, first used Qubit2.0 for preliminary quantification, diluted the library to 1 ng/μL, and then used Agilent 2100 to detect the insert size of the library, and qPCR to accurately quantify the effective concentration of the library (the effective concentration of the library>2 nM). The different libraries were sequenced after pooling according to the requirements of effective concentration and target data volume.

2.13. Statistical analysis

All data are shown as the mean values ± standard deviation of the mean (SD). Imaging comparisons and western blotting data were analyzed across groups with a one-way ANOVA with Tukey's multiple comparisons post-test. All the analysis and statistics were performed using GraphPad Prism Version 6.0. In all cases, a p value less than or equal to 0.05 was considered as statistically significant.

3. Result

3.1. TBI promoted callus formation at the tibia fracture site

X-ray visually show the formation of callus and healing of tibia fractures between groups while Micro-CT could quantitatively compare fracture healing parameters through three-dimensional reconstruction. X-rays at 3 and 5 weeks postoperatively indicated that the fracture lines of the tibia specimens in both groups were blurred, accompanied by a large amount of callus growth at the fracture site. 3 weeks after surgery, the TF group had more callus than the SF group, but there was no significant difference in the amount of callus between the two groups at 5 weeks. The trend of Micro-CT is consistent with X-ray (Fig. 1A and B). At 3 weeks postoperatively, the BV, TV and Tb.N values of the TF group were significantly higher than those of the SF group. Although the BV/TV value was not statistically significant, the mean value of the TF group was higher than that of the SF group. At 5 weeks after surgery, there was no significant difference in BV, TV, BV/TV and Tb.N values between the two groups (Fig. 1C–F).

Histopathological examination of tibial specimens was performed to observe the morphology of bone tissue and detect the expression of

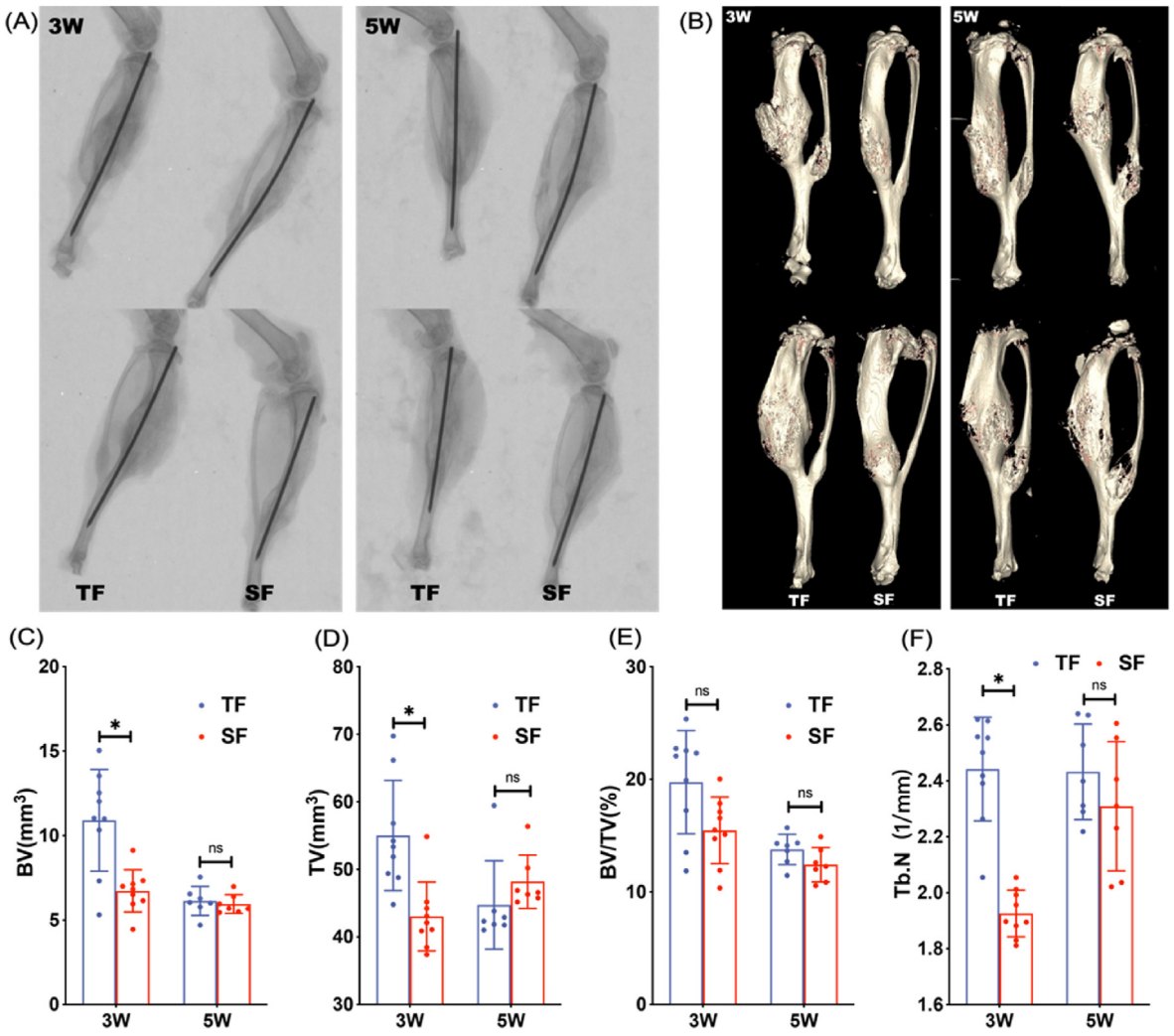

Figure 1. Representative X-ray (A) and Micro-CT (B) images of mice in TF and SF groups at 3 and 5 weeks after modeling (C–F) Quantitative analysis of fracture healing parameters (BV, TV, BV/TV, and Tb.N) of mice in TF and SF groups at 3 (n = 9 in each group) and 5 (n = 7 in each group) weeks after modeling (*$p < 0.05$).

osteogenic markers. HE staining showed that 3 weeks after the operation, a large number of disorderly and dense trabeculae were seen in the callus of the TF group with the surface covered with many short columnar, single-row arranged osteoblasts (yellow dotted curve, Fig. 2A), while the trabecular bone in the SF group is looser and the amount of osteoblasts is less than that in the TF group.

RUNX2 and Osterix are transcription factors necessary for osteoblast differentiation and the latter is specifically expressed only in developing bone tissue. Immunohistochemical results showed that a large number of RUNX2 and Osterix positive expression factors scattered in the trabecular bone were found in the callus of the TF group at 3 weeks after operation, while the expression of the two factors in the SF group was less. 5 weeks after surgery, both factors in the TF group and the SF group were expressed in small amounts near the surface of the callus (Fig. 2B–E).

3.2. Exosomes derived from plasma in TF group promoted osteoblast proliferation

Exosomes were extracted by ultracentrifugation after collecting blood samples at three time points: 1, 3, and 7 days after surgery. Then the exosomes were identified by transmission electron microscopy, particle size analysis and Western Blot. Under the transmission electron microscope, a saucer type with a diameter of about 100 nm or a hemispherical substance with a concave side were seen (Fig. 3A). The particle size analysis showed that the sample size is concentrated at about 100 nm (Fig. 3B), and Western Blot also detected exosome-marking proteins TSG101 and CD9 (Fig. 3C). The above results confirmed that we had successfully extracted exosomes and could be used in subsequent experiments.

Exosomes were extracted from the same volume of plasma in each group on the 1, 3, and 7 days after modeling. The results showed that the amount of exosomes was the largest on 1 day, compared with the amount on 3 and 7 days, the difference was statistically significant ($p < 0.01$) (Fig. 4A). CCK-8 was used to detect cell proliferation, and it was found that cell proliferation in the TF1 group no longer increased significantly after 24 h (Fig. 4B). The proliferation of MC3T3-E1 cells was detected after co-cultured with exosomes for 24 h in each group. The results showed that the exosomes in TF1 group had the strongest effect in promoting the proliferation of MC3T3-E1 cells, and the difference was statistically significant compared with the SF1 group ($p < 0.05$) (Fig. 4C).

3.3. Exosomes derived from plasma in TF group enhanced osteogenetic activity of osteoblast

COL1A1 and RUNX2 are specific markers reflecting osteoblast activity and bone formation. After co-cultured with exosomes in each group for 1 week, the MC3T3-E1 cells were assayed for osteogenic differentiation by measuring the expression of osteogenic proteins using western blot and q-PCR. Fig. 5A–B showed that the mRNA expression levels of COL1A1 and RUNX2 genes in the TF1 group were significantly higher

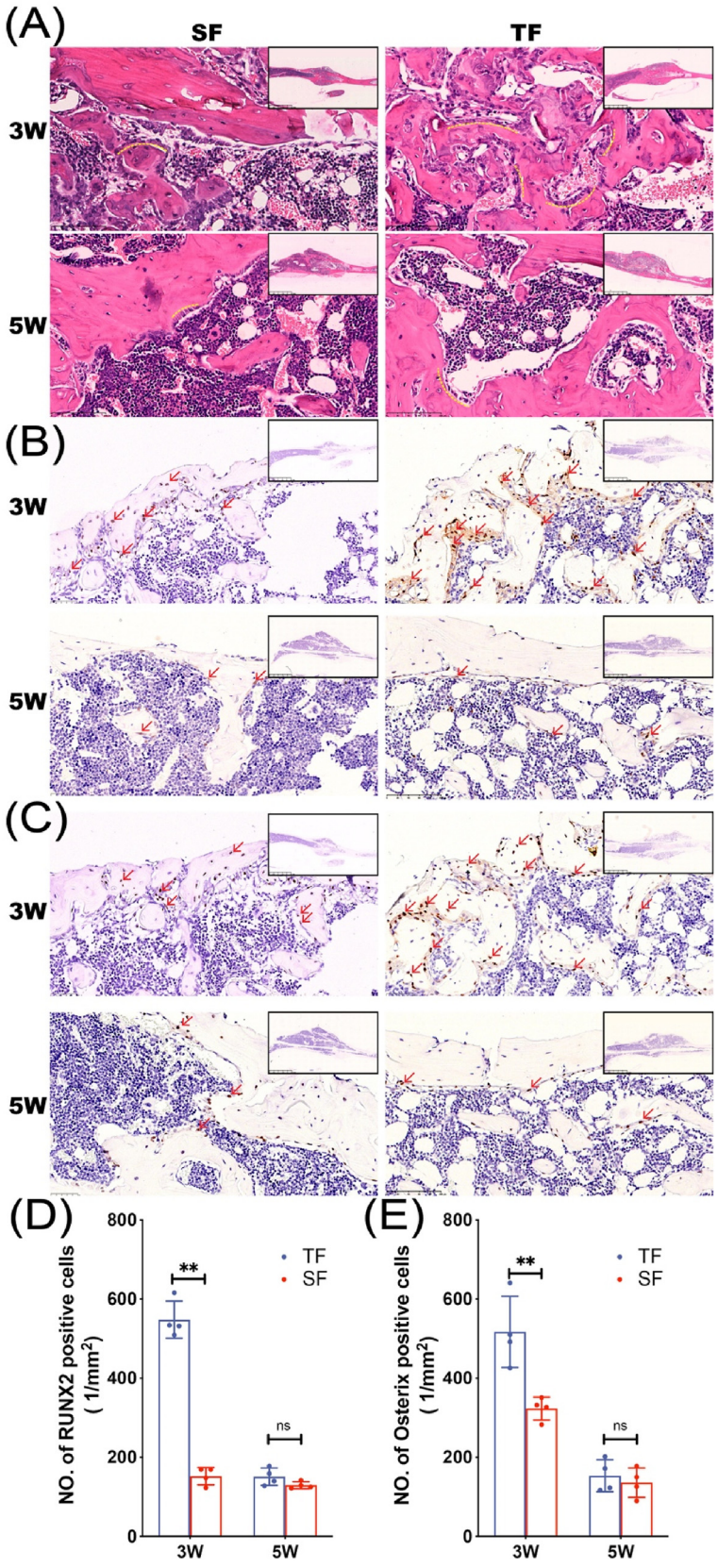

Figure 2. Histopathology differences of mice in TF group and SF group 3 and 5 weeks after modeling (A) H&E staining of fracture specimens in each group. RUNX2 (B) and Osterix (C) immunohistochemical staining of fracture specimens from TF and SF groups (D–E) Quantitative analysis of RUNX2 and Osterix positive cells (n = 4 in each group, $^{**}p < 0.01$) Red arrows indicate RUNX2 and Osterix positive cells.

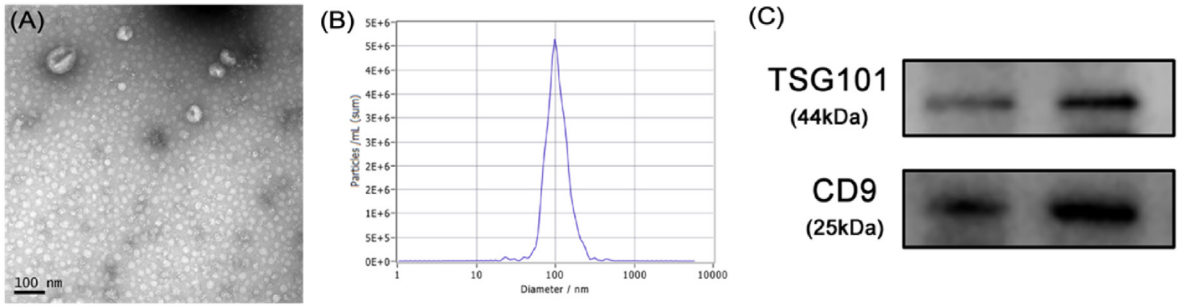

Figure 3. Identification of exosomes (A) Circular membrane-like structures with diameters of about 100 nm under transmission electron microscopy (B) The sample size is concentrated at about 100 nm (C) Western-blotting for exosome markers, TSG101and CD9.

than those in the SF1 group (both $p < 0.01$) (Fig. 5A–B). Besides, Fig. 5C–F showed an increased expression of the COL1A1 and RUNX2 protein in TF1 group compared to those in SF1 group (both $P < 0.01$) (Fig. 5C–F). Immunofluorescence was also performed to compare the expression of COL1A1 and RUNX2 proteins in each group. The results showed that the protein expression of COL1A1 and RUNX2 in the TF1 group was significantly higher than that in the SF1 group (both $p < 0.01$) (Fig. 5G–H).

After 2 weeks, the cells were stained with Alizarin Red to compare the matrix mineralization of the cells in each group. The results showed that the matrix mineralization in TF1 group was significantly enhanced than in SF1 group ($p < 0.01$) (Fig. 6).

3.4. miRNAs in exosomes derived from plasma in TF group had a potential role in promoting osteogenic activity

Mouse plasma exosome miRNAs were sequenced. Different colors represent different miRNA expression levels, and the colors from blue to red represent the expression level from low to high. Red indicates highly expressed genes, and dark blue indicates low expressed genes. Data processing screened to obtain 14 miRNAs that were highly expressed in the TBI group (TF group and T group) and low expressed in the non-TBI group (NOR group and SF group), namely: miR-148a-3p, miR-9182_L-4, miR-5121_L-1R+3, miR-125b-1-3p, miR-154–5p, miR-29a-5p_R-1, miR-34a-5p, miR-378a-5p, miR-22–3p, miR-149–5p_R-3, miR-4508_L+2R-1, miR-455–5p, miR-378c_R-1, miR-378a-3p_R-1 (Fig. 7A). Among them, we selected miR-22–3p, miR-34a-5p, and miR-378a-3p to verify their ability to promote osteogenic differentiation. We induced the transfected MC3T3-E1 cells to undergo osteogenic differentiation and stained with Alizarin Red 2 weeks later to compare the matrix mineralization of the cells in each group. The results showed that the matrix mineralization of miR-22–3p group, miR-34a-5p group, and miR-378a-3p group were significantly enhanced than that of CTRL, miR-NC group (Fig. 7B–C, $p < 0.01$).

4. Discussion

In this experiment, we extracted exosomes from plasma as the research object. First, a mouse model of tibia fracture combined with TBI was established. Plasma was collected on days 1, 3, and 7, and exosomes were extracted by ultracentrifugation. Exosomes were identified by transmission electron microscopy, particle size analysis and western blotting. It was found that the concentration of exosomes was the highest on the 1st day after modeling. CCK-8 detection showed that cell proliferation in TF1 group no longer increased after 24 h, and it indicated that the exosomes in TF1 group had the strongest effect in promoting the proliferation of MC3T3-E1 cell. After co-cultured with exosomes in each group for 1 week, the MC3T3-E1 cells were assayed for osteogenic differentiation by measuring the expression of osteogenic proteins using immunofluorescence, western blot and q-PCR. The results showed that the expressions of COL1A1 and RUNX2 in TF1 group were significantly higher than those in SF1 group. Alizarin Red Staining was used to compare the mineralization of cell matrix in each group. The results showed that the matrix mineralization of TF1 group was significantly enhanced than that of SF1 group. We performed miRNA sequencing on plasma exosomes in each group, and screened out miRNAs with high expression in the TBI groups and low expression in the non-TBI groups. Three of the miRNAs were transfected into MC3T3-E1 cells, and then subjected to osteogenic differentiation and stained with Alizarin Red. The results showed that the cell matrix mineralization of miR-22–3p, miR-34a-5p, miR-378a-3p transfection groups were significantly enhanced than that of CTRL group. Our experimental results show that plasma exosomes after TBI have the ability to promote osteoblast differentiation.

Among the many factors affecting the prognosis of complex fractures in patients with multiple injuries, the mechanism of action of traumatic brain injury (TBI) continues to be an intriguing topic. Surgeons found that patients with fractures and brain trauma healed faster than patients with a single fracture, and the growth of the callus at the end of the fracture was more abundant [10,11]. In order to investigate whether TBI will affect the prognosis of peripheral bone fractures, we developed a new multi-trauma mouse model, including weight-drop TBI and tibia fracture. In the process of TBI modeling, we found that different degrees of TBI have different effects on fracture healing. Mild TBI has no obvious effect on fracture healing, while moderate and severe TBI can promote fracture healing. However, severe TBI is very easy to cause the death of mice, so we control the weight and height of the free fall weight to make a moderate TBI model of mice. The method of making the tibia fracture model is relatively mature. In this experiment, the posterior patellar ligament was selected as the intramedullary nail insertion point, which improved the success of the puncture, and could avoid excessive peeling of soft tissue and reduce additional trauma. The selection of the transverse position of the middle tibia of the fracture site reduced the deviation of the fracture position selection. At the same time, this position does not exceed the distal tibiofibular joint, which also plays a certain role in the stability of the tibia fracture. Through X-ray and micro CT, fracture healing following tibial osteotomy with external fixation and additional TBI was characterized by increased callus formation and the gradual formation of bone bridges.

In recent years, bone tissue engineering studies have combined exosomes with scaffolds, revealing the active role of exosomes in bone regeneration [12–15]. Liu et al. found that lithium-containing bioactive scaffold (Li-BGC) promotes the angiogenesis of HUVECs by stimulating the secretion of exosome miR-130a derived from bone marrow stromal cells [13]. Wei et al. demonstrated that exosomes coated with titanium nanotubes can promote the osteogenic differentiation of human bone marrow mesenchymal stem cells [14]. Exosomes act like extracellular carriers, transferring lipids, proteins, and miRNAs from donor cells to recipient cells, thereby affecting the function of target cells. Exosomes from different cells can regulate the function of osteoblasts. BMSC-derived exosomes have a therapeutic effect on bone loss in rats during the repair of damaged osteoblast differentiation. Intravenous

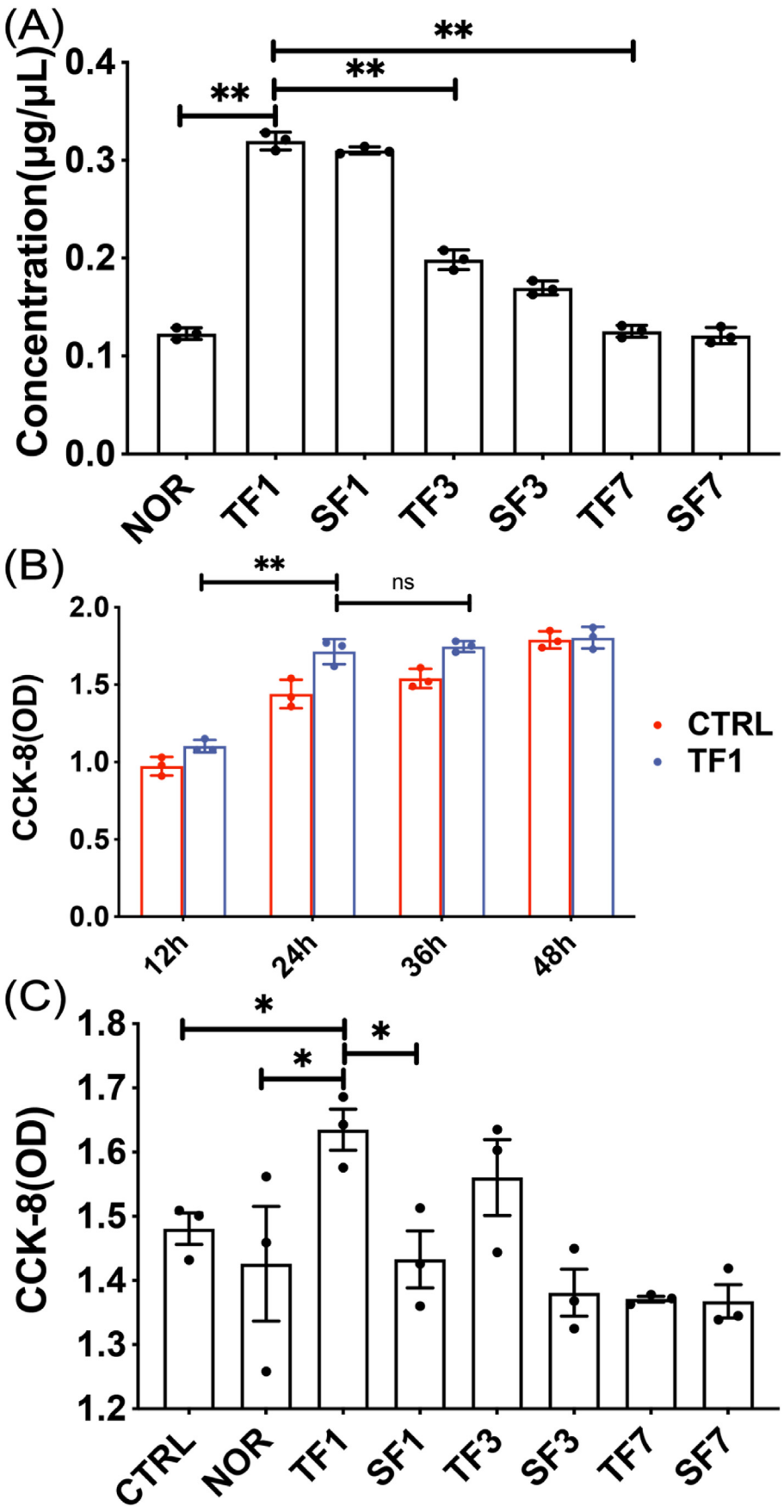

Figure 4. The effect of exosomes on the proliferation of MC3T3-E1 cells (A) The concentration of exosomes extracted at different time points (B) The time gradient of the effect of exosomes on the proliferation of MC3T3-E1 cells (C) Cell proliferation of each group of exosomes co-cultured with MC3T3-E1 cells for 24 h. CTRL: without exosomes intervention; NOR: exosomes extracted from normal mice. TF1, TF3, TF7: exosomes extracted on the 1st, 3rd and 7th day after TBI combined with left tibia fracture modeling. SF1, SF3, SF7: exosomes extracted on the 1st, 3rd and 7th day after sham-TBI combined with left tibia fracture modeling (*$p < 0.05$).

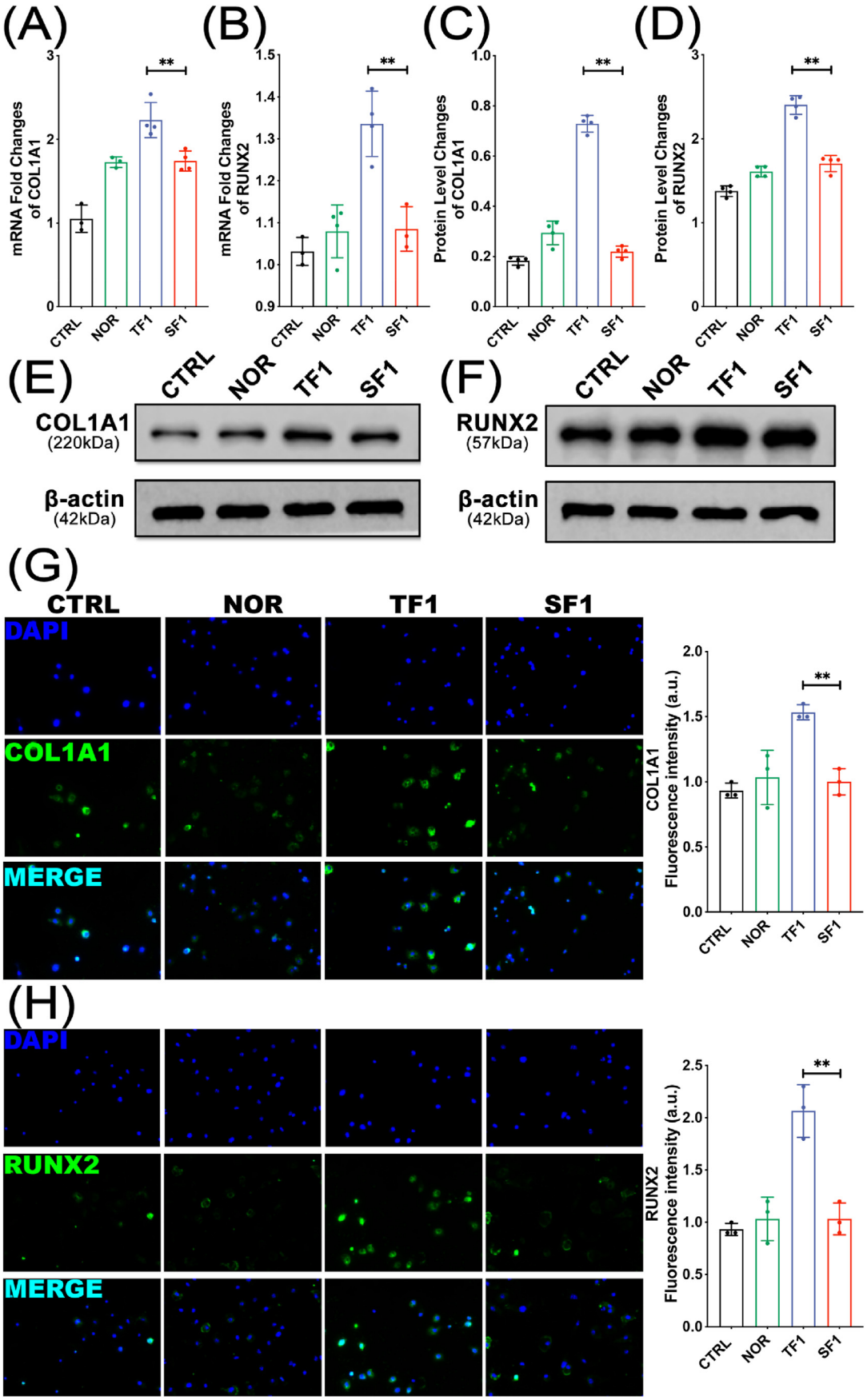

Figure 5. The mRNA and protein expression levels of COL1A1 and RUNX2 (A–B) qPCR analysis of COL1A1 and RUNX2 mRNA expression levels (C–F) Western blotting bands and quantification of COL1A1 and RUNX2 (G–H) Representative immunofluorescence images and quantification analysis of COL1A1 and RUNX2 (**$p < 0.01$).

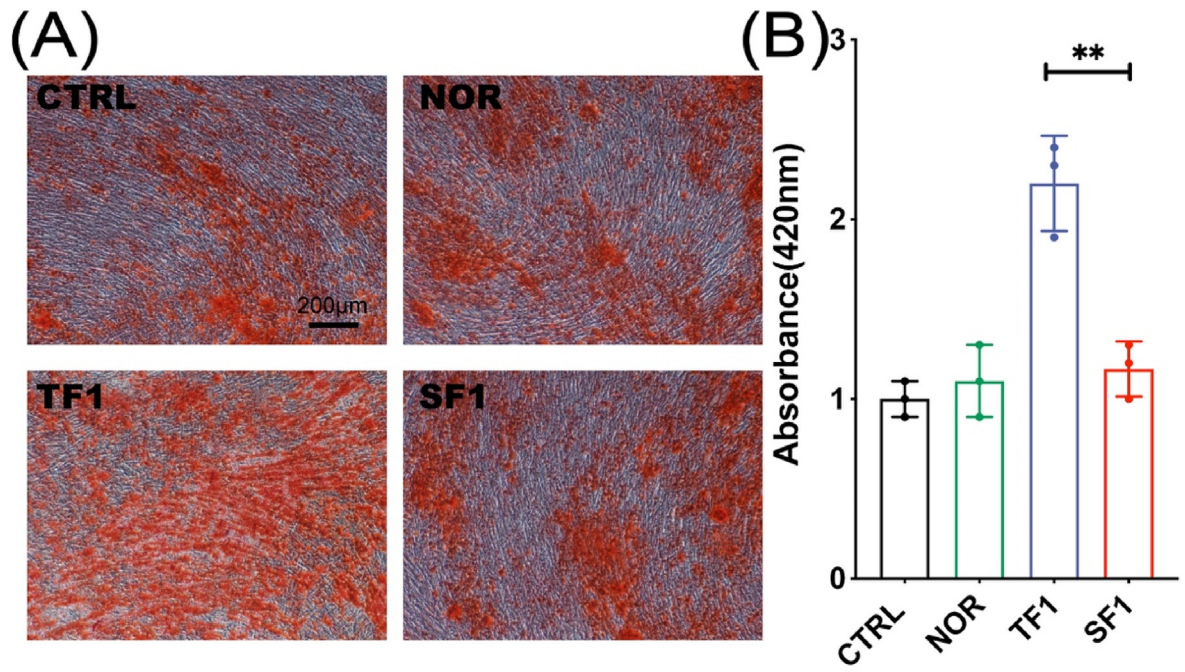

Figure 6. The matrix mineralization and quantification analysis after osteogenic differentiation under Alizarin Red staining. (A) Representative Alizarin Red staining images. (B) Quantification analysis of OD values of the destained solution from above cells staining. (** $p<0.01$).

injection of exosomes derived from bone marrow stromal stem cells can reduce bone loss. At the same time, exosome treatment increased calcium deposition at the mRNA and protein levels and expression of the osteogenic gene RUNX2 compared to the untreated group [16]. Studies have found that exosomes extracted from MC3T3 mouse osteoblasts contain a large number of proteins that are highly enriched in osteogenic signaling pathways, such as eukaryotic initiation factor 2 signaling pathway, integrin signaling pathway and mTOR signaling pathway [7]. Another study showed that MC3T3 mouse osteoblasts can release exosomes containing osteogenic miRNAs, which are taken up by mouse bone marrow-derived stromal ST2 cells, thereby promoting the osteoblast differentiation of the receptor ST2 cells [17]. At the same time, osteoclast precursor monocytes were also found to have the ability to release exosomes. Li et al. reported that osteoclasts release exosomes containing miR-214–3p, which can be transferred to osteoblasts and inhibit osteoblast activity and bone formation [18]. Osteoclast-derived exosomes participate in the communication between osteoclasts and osteoblasts.

The blood–brain barrier is a complex system composed of brain microvascular endothelial cells, astrocytes, pericytes, macrophages around blood vessels, and basement membrane. Patients with brain trauma often have blood–brain barrier damage and dysfunction [19]. When brain trauma occurs, the function of the blood–brain barrier changes significantly. The permeability of the blood–brain barrier increases, while the large osteogenic molecules in the central nervous system are released from the damaged brain tissue and act on the fracture through the systemic circulation [20,21]. Proteomics studies have shown that the response of serum and cerebrospinal fluid proteins to TBI has changed, which may be related to the osteogenic effect of TBI on fracture healing [22]. Bidner et al. found that, compared with patients with no TBI, the serum of patients with TBI can increase the proliferation of fetal rat skull cells [20]. Boes et al. found that compared with the serum of rats with simple fractures, the mixed serum of TBI and fractured rats can increase the proliferation of mesenchymal stem cells, but not the proliferation of fibroblasts or osteoblast cell lines [23].

There is increasing evidence that miRNAs play a key role in bone reconstruction. miRNA has become an important post-transcriptional regulator of bone formation and bone resorption. Serum exosome miR-214–3p increased in elderly fracture patients. Exosome miR-214–3p can prevent osteoblast differentiation and bone formation [18]. In 175 patients with recent osteoporotic fractures of the femoral neck, there are 6 miRNAs (miR-10a-5p, miR-10b-5p, miR-22–3p, miR-133b, miR-328–3p, let-7g-5p) different from the control group. The first three miRNAs are up-regulated, and the last three miRNAs are down-regulated [24], revealing that exosome miRNAs play a crucial role in identifying osteogenic differentiation. In this experiment, we performed miRNA sequencing on the isolated exosomes, and further screened the data to obtain 14 miRNAs that were highly expressed in the TBI group and lowly expressed in the non-TBI group. Through literature search, we found that miR-22–3p, miR-34a-5p, miR-378a-3p, miR-146a-5p and miR-342–3p have the effect of promoting osteoblast differentiation [25–28], while miR-125b-1-3p, miR-154–5p and miR-375–3p have the effect on inhibiting the differentiation of osteoblast [29–31], and miR-148a-3p, miR-378a-5p and miR-378c have the effect of promoting the osteoclasts differentiation [32,33]. In our study, we also verified that miR-22–3p, miR-34a-5p, and miR-378a-3p have the ability to promote osteoblast differentiation, consistent with the results reported in the literatures. However, the effects of other miRNA candidates need to be investigated in the future research. In summary, exosomes may promote fracture healing by delivering miRNA to the fracture end, promoting osteoblast differentiation or inhibiting osteoclast differentiation.

Although TBI can promote the healing of fractures, heterotopic ossification is an important issue that cannot be ignored. Heterotopic ossification (HO) is a pathological phenomenon that forms mature bone in the soft tissue outside the bone [34]. The disease is usually caused by fractures, burns, nervous system damage (brain damage and spinal cord injury) and joint replacement. Patients with HO may have symptoms such as tissue swelling, inflammation, pain, restricted mobility, and joint adhesions, which significantly affect patients' lives and emotions [35,36]. There are three types of HO, namely progressive ossifying myositis, traumatic HO and neurological HO [37]. In theory, HO may occur in any part of the body, but in most cases, it occurs in joints such as the hips, elbows, and shoulders [38]. Recent studies have found that patients with fractures and severe TBI have a significantly increased risk of HO [39]. The incidence of neurogenic heterotopic ossification (NHO) in patients with TBI is about 20%, but when TBI and femoral fractures occur at the same time, the incidence of NHO exceeds 50% [37]. Fracture healing and

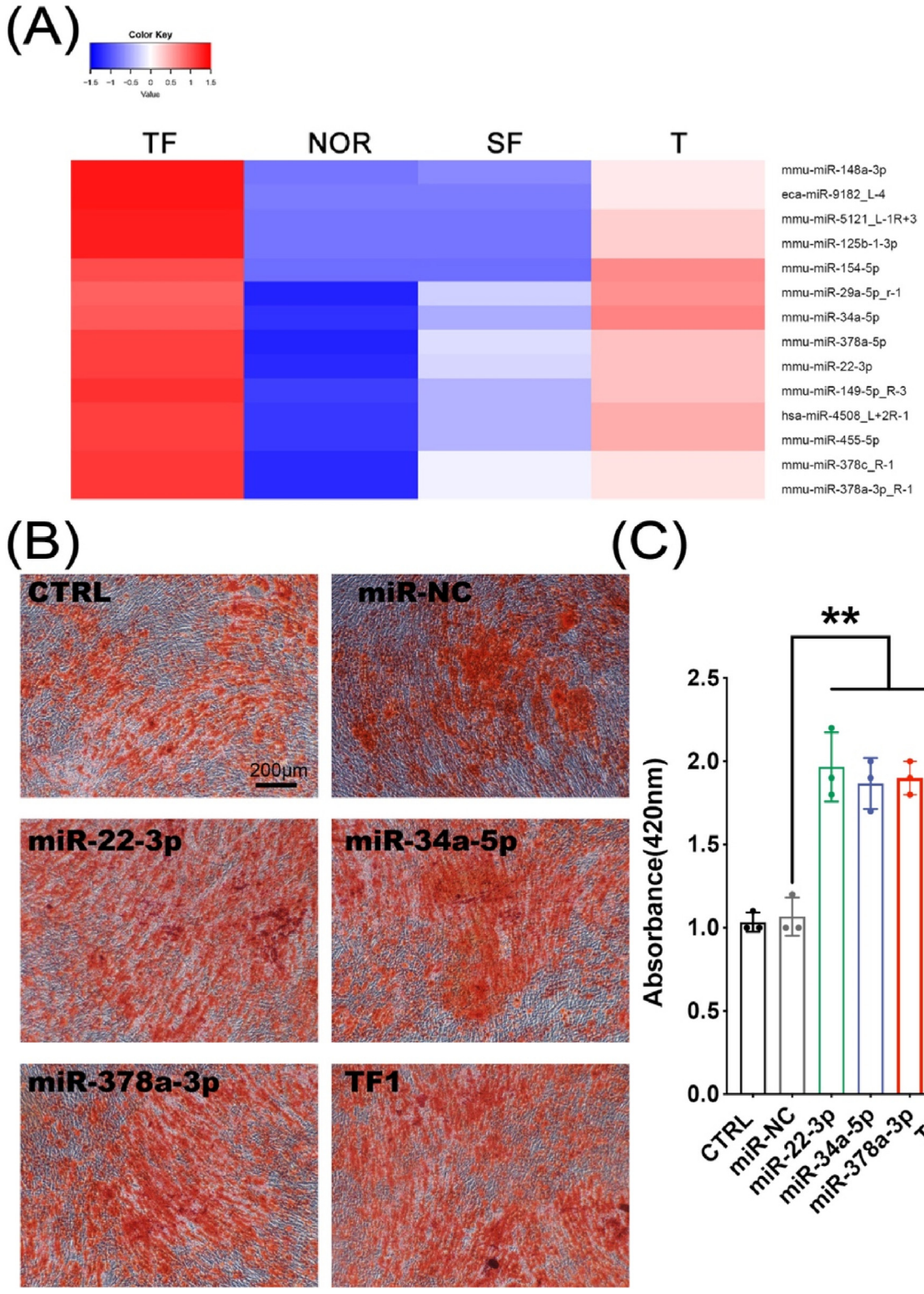

Figure 7. (A) Highly expressed in the TBI group (TF group and T group) and low expressed in the non-TBI group (NOR group and SF group) (B–C) The matrix mineralization and quantification of cells after osteogenic differentiation under Alizarin Red staining (**p < 0.01).

HO have common initial events (inflammation, angiogenesis, chondrogenesis and bone formation) [40]. Indeed, fractures can in turn stimulate the release of inflammatory cytokines and aggravate TBI symptoms. Study showed that chronic fractures occurred 4 days after craniocerebral injury. The volume of brain injury and brain water content increased significantly, which was related to fractures. It is worth noting that the stimulation of the immune system by fractures can significantly promote the release of various inflammatory factors, such as TNF-a, IL-1b, and IL-6 are all increased [41]. Also in C57BL/6J mice, TBI with fractures resulted in increased levels of various body fluid inflammatory cytokines [42].

In summary, this study used a mouse model of TBI combined with tibia fractures, to investigate the impact of TBI as a factor conducive to

fracture healing. Plasma exosomes early after TBI have the ability to promote osteoblast differentiation. The mechanism may be achieved by miRNA in exosomes. Plasma exosomes can be used as breakthrough clinical treatment for delayed or non-union fractures.

However, this study has several limitations. First, the source of exosomes in plasma has not been traced. Second, the mechanism by which exosomes promote the proliferation and differentiation of osteoblasts has not been clarified. Further research is needed to clarify the relationship between TBI and fractures. Finally, the translation of natural exosomes to the clinic is often limited due to the lack of scalable isolation and effective drug loading methods. Alternative strategy to use exosomes for clinical treatment is to develop exosome mimics. Liposomes are synthetic, spherical vesicles with bilayer lipid molecules, ranging in diameter from 25 to 1000 nm. Liposome has the characteristics of good biocompatibility, biodegradability and non-immunogenicity, and is an excellent drug carrier. At present, it has been widely used in anti-tumor drugs, antifungal drugs, antibiotic drugs, etc. However, they are often criticized for short blood circulation and low intracellular drug delivery efficiency. Exosome-mimicking liposomes, which exhibit significantly higher cellular uptake and intracellular delivery efficiency than traditional liposomes, could be envisioned for promoting fracture healing in future.

Conflict of interest statement

All the authors declare that the research was conducted in the absence of any commercial or financial relationships which could be construed as a potential conflict of interest.

Funding

This work was supported by the National Natural Science Foundation of China (81871789, 82172387, 81702214, 81802200), the Natural Science Foundation of Jiangsu Province (BK20180052), and Gusu Health Talents Program (GSWS2020023), Suzhou Municipal Science and Technology Bureau (SYS2019018) and the General Project of Suzhou Vocational Health College (szwzy201907).

Ethics statement

All experiment procedures involved in this study strictly abided by the recommendations in the Guide for the Care and Use of Laboratory Animals of the National Institutes of Health and were approved by the Committee on the Ethics of Animal Experiments of The First Affiliated Hospital of Soochow University (Suzhou, China).

Declaration of competing interest

The authors declare no potential conflicts of interest.

References

[1] Hofman M, Koopmans G, Kobbe P, Poeze M, Andruszkow H, Brink PR, et al. Improved fracture healing in patients with concomitant traumatic brain injury: proven or not? Mediat Inflamm 2015;2015:204842. https://doi.org/10.1155/2015/204842. Epub 202015 Mar 204822.

[2] Bajwa NM, Kesavan C, Mohan S. Long-term consequences of traumatic brain injury in bone metabolism. Front Neurol 2018;9:115. https://doi.org/10.3389/fneur.2018.00115. eCollection 02018.

[3] Mollahosseini M, Ahmadirad H, Goujani R, Khorramdelazad H. The association between traumatic brain injury and accelerated fracture healing: a study on the effects of growth factors and cytokines. J Mol Neurosci 2020;7(10):20–1640.

[4] Wildburger R, Zarkovic N, Egger G, Petek W, Zarkovic K, Hofer HP. Basic fibroblast growth factor (BFGF) immunoreactivity as a possible link between head injury and impaired bone fracture healing. Bone Miner 1994;27(3):183–92. 110.1016/s0169-6009(1008)80192-80194.

[5] Zhang R, Liang Y, Wei S. The expressions of NGF and VEGF in the fracture tissues are closely associated with accelerated clavicle fracture healing in patients with traumatic brain injury. Therapeut Clin Risk Manag 2018;14:2315–22. https://doi.org/10.2147/TCRM.S182325. eCollection 182018.

[6] Théry C, Zitvogel L, Amigorena S. Exosomes: composition, biogenesis and function. Nat Rev Immunol 2002;2(8):569–79. 510.1038/nri1855.

[7] Ge M, Ke R, Cai T, Yang J, Mu X. Identification and proteomic analysis of osteoblast-derived exosomes. Biochem Biophys Res Commun 2015;467(1):27–32. https://doi.org/10.1016/j.bbrc.2015.1009.1135. Epub 2015 Sep. 1028.

[8] Deng L, Wang Y, Peng Y, Wu Y, Ding Y, Jiang Y, et al. Osteoblast-derived microvesicles: a novel mechanism for communication between osteoblasts and osteoclasts. Bone 2015;79:37–42. https://doi.org/10.1016/j.bone.2015.1005.1022. Epub 2015 May 1024.

[9] Huynh N, VonMoss L, Smith D, Rahman I, Felemban MF, Zuo J, et al. Characterization of regulatory extracellular vesicles from osteoclasts. J Dent Res 2016;95(6):673–9. 610.1177/0022034516633189. Epub 0022034516632016 Feb 0022034516633123.

[10] Perkins R, Skirving AP. Callus formation and the rate of healing of femoral fractures in patients with head injuries. J Bone Joint Surg Br 1987;69(4):521–4.

[11] Huang W, Li Z, Li Z, Yang R. Does traumatic brain injury result in accelerated mandibular fracture healing? J Oral Maxillofac Surg 2012;70(9):2135–42. 2110.1016/j.joms.2012.2104.2016.

[12] Qi X, Zhang J, Yuan H, Xu Z, Li Q, Niu X, et al. Exosomes secreted by human-induced pluripotent stem cell-derived mesenchymal stem cells repair critical-sized bone defects through enhanced angiogenesis and osteogenesis in osteoporotic rats. Int J Biol Sci 2016;12(7):836–49. 810.7150/ijbs.14809. eCollection 12016.

[13] Liu L, Liu Y, Feng C, Chang J, Fu R, Wu T, et al. Lithium-containing biomaterials stimulate bone marrow stromal cell-derived exosomal miR-130a secretion to promote angiogenesis. Biomaterials 2019;192:523–36. https://doi.org/10.1016/j.biomaterials.2018.1011.1007. Epub 2018 Nov 1018.

[14] Wei F, Li M, Crawford R, Zhou Y, Xiao Y. Exosome-integrated titanium oxide nanotubes for targeted bone regeneration. Acta Biomater 2019;86:480–92. https://doi.org/10.1016/j.actbio.2019.1001.1006. Epub 2019 Jan 1017.

[15] Li W, Liu Y, Zhang P, Tang Y, Zhou M, Jiang W, et al. Tissue-engineered bone immobilized with human adipose stem cells-derived exosomes promotes bone regeneration. ACS Appl Mater Interfaces 2018;10(6):5240–54. 5210.1021/acsami.5247b17620. Epub 12018 Feb 17622.

[16] Zuo R, Liu M, Wang Y, Li J, Wang W, Wu J, et al. BM-MSC-derived exosomes alleviate radiation-induced bone loss by restoring the function of recipient BM-MSCs and activating Wnt/β-catenin signaling. Stem Cell Res Ther 2019;10(1):30. https://doi.org/10.1186/s13287-13018-11121-13289.

[17] Cui Y, Luan J, Li H, Zhou X, Han J. Exosomes derived from mineralizing osteoblasts promote ST2 cell osteogenic differentiation by alteration of microRNA expression. FEBS Lett 2016;590(1):185–92. 110.1002/1873-3468.12024. Epub 12015 Dec 12030.

[18] Li D, Liu J, Guo B, Liang C, Dang L, Lu C, et al. Osteoclast-derived exosomal miR-214-3p inhibits osteoblastic bone formation. Nat Commun 2016;7:10872. https://doi.org/10.1038/ncomms10872.

[19] Shlosberg D, Benifla M, Kaufer D, Friedman A. Blood-brain barrier breakdown as a therapeutic target in traumatic brain injury. Nat Rev Neurol 2010;6(7):393–403. 310.1038/nrneurol.2010.1074. Epub 2010 Jun 1015.

[20] Bidner SM, Rubins IM, Desjardins JV, Zukor DJ, Goltzman D. Evidence for a humoral mechanism for enhanced osteogenesis after head injury. J Bone Joint Surg Am 1990;72(8):1144–9.

[21] Başkaya MK, Rao AM, Doğan A, Donaldson D, Dempsey RJ. The biphasic opening of the blood-brain barrier in the cortex and hippocampus after traumatic brain injury in rats. Neurosci Lett 1997;226(1):33–6. https://doi.org/10.1016/s0304-3940(1097)00239-00235.

[22] Cadosch D, Thyer M, Gautschi OP, Lochnit G, Frey SP, Zellweger R, et al. Functional and proteomic analysis of serum and cerebrospinal fluid derived from patients with traumatic brain injury: a pilot study. ANZ J Surg 2010;80(7–8):542–7. 510.1111/j.1445-2197.2010.05268.x.

[23] Boes M, Kain M, Kakar S, Nicholls F, Cullinane D, Gerstenfeld L, et al. Osteogenic effects of traumatic brain injury on experimental fracture-healing. J Bone Joint Surg Am 2006;88(4):738–43. 710.2106/JBJS.D.02648.

[24] Weilner S, Skalicky S, Salzer B, Keider V, Wagner M, Hildner F, et al. Differentially circulating miRNAs after recent osteoporotic fractures can influence osteogenic differentiation. Bone 2015;79:43–51. https://doi.org/10.1016/j.bone.2015.1005.1027. Epub 2015 May 1028.

[25] Wang G, Zhao F, Yang D, Wang J, Qiu L, Pang X. Human amniotic epithelial cells regulate osteoblast differentiation through the secretion of TGFβ1 and microRNA-34a-5p. Int J Mol Med 2018;41(2):791–9. 710.3892/ijmm.2017.3261. Epub 2017 Nov 3817.

[26] Krist B, Florczyk U, Pietraszek-Gremplewicz K, Józkowicz A, Dulak J. The role of miR-378a in metabolism, angiogenesis, and muscle biology. Internet J Endocrinol 2015;2015:281756. https://doi.org/10.1155/2015/281756. Epub 282015 Dec 281729.

[27] Li P, Sun N, Zeng J, Zeng Y, Fan Y, Feng W, et al. Differential expression of miR-672-5p and miR-146a-5p in osteoblasts in rats after steroid intervention. Gene 2016;591(1):69–73. https://doi.org/10.1016/j.gene.2016.1006.1045. Epub 2016 Jul 1011.

[28] Huang M, Qing Y, Shi Q, Cao Y, Song K. miR-342-3p elevates osteogenic differentiation of umbilical cord mesenchymal stem cells via inhibiting Sufu in vitro. Biochem Biophys Res Commun 2017;491(3):571–7. 510.1016/j.bbrc.2017.1007.1163. Epub 2017 Jul 1029.

[29] Vasanthan P, Govindasamy V, Gnanasegaran N, Kunasekaran W, Musa S, Abu Kasim NH. Differential expression of basal microRNAs' patterns in human dental pulp stem cells. J Cell Mol Med 2015;19(3):566–80. 510.1111/jcmm.12381. Epub 12014 Dec 12385.

[30] Li J, Hu C, Han L, Liu L, Jing W, Tang W, et al. MiR-154-5p regulates osteogenic differentiation of adipose-derived mesenchymal stem cells under tensile stress through the Wnt/PCP pathway by targeting Wnt11. Bone 2015;78:130–41. https://doi.org/10.1016/j.bone.2015.1005.1003. Epub 2015 May 1017.
[31] Sun T, Li CT, Xiong L, Ning Z, Leung F, Peng S, et al. miR-375-3p negatively regulates osteogenesis by targeting and decreasing the expression levels of LRP5 and β-catenin. PloS One 2017;12(2):e0171281. 0171210.0171371/journal.pone.0171281. eCollection 0172017.
[32] Kelch S, Balmayor ER, Seeliger C, Vester H, Kirschke JS, van Griensven M. miRNAs in bone tissue correlate to bone mineral density and circulating miRNAs are gender independent in osteoporotic patients. Sci Rep 2017;7(1):15861. 15810.11038/s41598-15017-16113-x.
[33] Kagiya T, Nakamura S. Expression profiling of microRNAs in RAW264.7 cells treated with a combination of tumor necrosis factor alpha and RANKL during osteoclast differentiation. J Periodontal Res 2013;48(3):373–85. 310.1111/jre.12017. Epub 12012 Oct 12018.
[34] Davies OG, Grover LM, Eisenstein N, Lewis MP, Liu Y. Identifying the cellular mechanisms leading to heterotopic ossification. Calcif Tissue Int 2015;97(5):432–44. 410.1007/s00223-00015-00034-00221. Epub 02015 Jul 00211.
[35] Ranganathan K, Loder S, Agarwal S, Wong VW, Forsberg J, Davis TA, et al. Heterotopic ossification: basic-science principles and clinical correlates. J Bone Joint Surg Am 2015;97(13):1101–11. 1110.2106/JBJS.N.01056.
[36] van Kuijk AA, Geurts AC, van Kuppevelt HJ. Neurogenic heterotopic ossification in spinal cord injury. Spinal Cord 2002;40(7):313–26. 310.1038/sj.sc.3101309.
[37] Morgan WE, Morgan CP. Chiropractic care of a patient with neurogenic heterotopic ossification of the anterior longitudinal ligament after traumatic brain injury: a case report. J Chiropr Med 2014;13(4):260–5. 210.1016/j.jcm.2014.1008.1001.
[38] Vanden Bossche L, Vanderstraeten G. Heterotopic ossification: a review. J Rehabil Med 2005;37(3):129–36. 110.1080/16501970510027628.
[39] Huang H, Cheng WX, Hu YP, Chen JH, Zheng ZT, Zhang P. Relationship between heterotopic ossification and traumatic brain injury: why severe traumatic brain injury increases the risk of heterotopic ossification. J Orthop Translat 2018;12:16–25. https://doi.org/10.1016/j.jot.2017.1010.1002. eCollection 2018 Jan.
[40] Ausk BJ, Gross TS, Bain SD. Botulinum toxin-induced muscle paralysis inhibits heterotopic bone formation. Clin Orthop Relat Res 2015;473(9):2825–30. 2810.1007/s11999-11015-14271-11994.
[41] Yang L, Guo Y, Wen D, Yang L, Chen Y, Zhang G, et al. Bone fracture enhances trauma brain injury. Scand J Immunol 2016;83(1):26–32. https://doi.org/10.1111/sji.12393.
[42] Probst C, Mirzayan MJ, Mommsen P, Zeckey C, Tegeder T, Geerken L, et al. Systemic inflammatory effects of traumatic brain injury, femur fracture, and shock: an experimental murine polytrauma model. Mediat Inflamm 2012;2012:136020. https://doi.org/10.1155/2012/136020. Epub 132012 Mar 136024.